

On the production mechanism of Σ -hypernuclear systems in $A(K^-, \pi^\pm)$ reactions

O.D.Dalkarov^a and V.M.Kolybasov^b

Lebedev Physical Institute, 117924 Moscow, Russia

Abstract

It is shown that the new data on the excitation energy E_{ex} spectrum of the residual nuclear system in the Σ -hypernuclear region in the reactions (K^-, π^\pm) on ${}^9\text{Be}$ and in the reaction (K^-, π^+) on ${}^4\text{He}$ and ${}^{12}\text{C}$ can be described without the supposition on the existence of excited Σ -hypernuclear states. The basis is formed by a simultaneous consideration of the quasi-free Σ -production and Σ -nuclear rescattering (elastic and with $\Sigma \rightarrow \Lambda$ conversion) with account of interference of the respective amplitudes. For final decision of the question about the nature of the irregularities in E_{ex} spectrum, it is proposed to study the picture corresponding to the so-called moving complex singularity of the triangle graph with Σ rescattering: the position and the width of the peak in E_{ex} distribution must appreciably change with momentum transferred from the initial kaon to the final pion.

PACS: 21.80.+a; 24.50.+g; 25.80.Nv

Keywords: Sigma-hypernuclear systems; Reaction mechanism; Moving singularities

^a e-mail: dalkarov@sci.lebedev.ru

^b e-mail: kolybasv@sci.lebedev.ru

1 Introduction

New BNL data on ${}^9\text{Be}(\text{K}^-, \pi^\pm)$ reactions at 600 MeV/c in Σ -hypernuclear region [1] drastically changed the situation around the problem of the existence of excited states of Σ -nuclei. As followed from the old data (see, for instance, review [2]) there were clear indications on the narrow peaks ($\Gamma < 10$ MeV) in the excitation energy spectrum of the residual nuclear systems in the region close to Σ -hyperon production. For this reason the idea about the creation of excited hypernuclear states seemed to be very attractive. However, from the very beginning the problem of a small hypernuclear width was discussed, since due to $\Sigma N \rightarrow \Lambda N$ conversion in nuclear matter all estimations lead to the widths more then $20 \div 40$ MeV [2,3]. Recent data (see Fig.1 where circles correspond to ${}^9\text{Be}(\text{K}^-, \pi^-)$ reaction and squares to ${}^9\text{Be}(\text{K}^-, \pi^+)$ one) exclude very narrow peaks but reveal the structures with the width about 20 MeV for (K^-, π^-) and $30 \div 40$ MeV for the case of (K^-, π^+) reaction.

Several questions should be cleared up: whether these peaks call for the idea about Σ -hypernuclei existence or they are caused by the reaction mechanism and, probably, by the nearthreshold phenomena? If it is possible to understand the problem without Σ -hypernuclei then how will the natural and doubtless description be made with the help of the simplest mechanisms? Finally, are there the crucial tests to clear the question about the nature of the irregularities in the excitation energy spectrum of Σ -hypernuclear systems? Below we will try to answer these questions.

The first goal of this study is to show that it is quite plausible to describe all of the data on the reaction ${}^9\text{Be}(\text{K}^-, \pi^-)$ and the reactions (K^-, π^+) on ${}^9\text{Be}$, ${}^{12}\text{C}$ and ${}^4\text{He}$ nuclei without the idea about the existence of excited Σ -hypernuclear states (see Fig.2d) but using Feynman graph language and

taking into account the quasi-free Σ -hyperon production (Fig.2a), the elastic rescattering of Σ (Fig.2b) and final inelastic interaction of Σ -hyperon with the $\Sigma \rightarrow \Lambda$ conversion (Fig.2c). In this case the interference of the pole graph of Fig.2a and the triangle graph of Fig.2b should be essential. We will also emphasize some characteristic features of the process ${}^9\text{Be}(K^-, \pi^+)$ distinguishing it against others.

Another and the main purpose is to advance theoretical apparatus for final revealing of the nature of the peaks in the excitation energy spectra in order to give a method which could allow to distinguish the peaks caused by the Σ -hypernuclei existence from ones produced by the reaction mechanism. This method is based on the analytical properties of Feynman graphs. In our case the singularities of the nonrelativistic triangle graph (see Fig.2e) are close to the physical region. This fact leads to the appearance of moving maxima in the excitation energy spectra as a function of the square of the momentum transferred from initial kaon to final π -meson. Note that in the experiment the extraction of this graph as a unique one is possible, if the Λ -hyperon, produced by the interaction of virtual Σ -hyperon with the intermediate nucleus, is detected. Therefore, the studying of the double differential cross sections (with and without Λ -hyperon detection in the final state) for $A(K, \pi)X$ reactions could be sufficient test to distinguish the main features of the reaction mechanism.

The paper is organized as follows. The theoretical model is described in Section 2. Kinematical relations between various differential cross sections are given and the detailed properties of the amplitude for the triangle graph are discussed. Section 3 is devoted to the procedure of ${}^9\text{Be}$ data processing, in particular, to a difference method which was used to extract the contribution of (K^-, π^-) process on the outer weakly bound neutron.

The question about the role of relative phase between the amplitudes for pole and triangle graphs (see Fig.2a and 2b) is also discussed.

The final results for (K^-, π^-) reaction on ${}^9\text{Be}$ and (K^-, π^+) one on ${}^9\text{Be}$, ${}^4\text{He}$ and ${}^{12}\text{C}$ nuclei, which are in good agreement with the experimental data, are given in Section 4. We also discuss possible reasons for strong difference between the excitation energy spectrum for ${}^9\text{Be}$ and the same ones for ${}^4\text{He}$ and ${}^{12}\text{C}$.

The picture of the moving triangle singularities is discussed in Section 5. We present results of the calculations for the excitation energy spectra for the channels with $\Sigma \rightarrow \Lambda$ conversion for different momentum transfer from initial kaon to final pion. They show that the moving peaks in the excitation energy spectra are experimentally observable. For comparison the excitation energy spectra with hypernuclear state production (see Fig.2d) are also calculated. In this case the position of the peak does not practically depend on the momentum transfer.

The main results and concluding remarks are given in Conclusion.

2 Theoretical model

We will consider the graphs of Fig.2a–2c where, as mentioned earlier, the pole graph (Fig.2a) represents quasi-free Σ -hyperon production. Triangle graphs correspond to the rescattering of virtual Σ on the intermediate nuclear system without conversion (Fig.2b) and with conversion (Fig.2c), excluding production of Σ -hypernuclear bound or resonance states (this process would correspond to the graph of Fig.2d). Let's analyze more accurately the main properties of triangle Feynman graphs before to make the fitting procedure. We will consider the general form of Fig.2e implying that the particle 2 is Σ -hyperon, and the particle 1 is the residual nuclear

system and the lower vertex stands in principle for the aggregate of all the processes that occur when Σ interacts with the residual nucleus. We denote by p_i and E_i the momentum and total energy of a particle i in the lab. system and introduce the notations

$$\mathbf{q} = \mathbf{p}_x - \mathbf{p}_z, \quad (1)$$

$$W = \sqrt{s_{12}} = [(m_A + E_x - E_z)^2 - q^2]^{1/2}.$$

Here W is the invariant mass of the system $4 + \dots n$, consisting of the particles produced after Σ -conversion in nuclear medium. We shall henceforth have relatively small q^2 only and W in the region where the Σ -hyperon 2 can be assumed with good accuracy to be nonrelativistic. If we neglect the complications that can appear when account is taken of the spin structure of the amplitudes and restrict ourself to the consideration of triangle diagram only (Fig.2e) then the quantity $d^2\sigma/dW dq^2$ can be expressed in terms of the differential cross section $d\sigma_{3x}/d\Omega$ of the elementary reaction $K^- + N \rightarrow \pi + \Sigma$ (in c.m.s. of this reaction) and the total cross section $\sigma_{12}(W)$ for the interaction of the Σ -hyperon and the nucleus 1 [4,5]:

$$\frac{d^2\sigma}{dW dq^2} = \frac{m_1^2 m_2 s_{3x}}{4\pi^3 m_3 (m_1 + m_2)^2 p_x^2} \kappa \gamma^2 \left(\frac{p_1^{cms}}{m_{12}} \sigma_{12}(W) \right) \left(\frac{\tilde{p}_x d\sigma_{3x}}{\tilde{p}_z d\Omega} \right) |M|^2 \quad (2)$$

Here $s_{3x} = m_3^2 + m_x^2 + 2m_3 E_x$, p_1^{cms} is the momentum of the relative motion of the particles 1 and 2 in the c.m.s. of particles $4 \dots n$, \tilde{p}_x and \tilde{p}_z are the momenta of particles x and z in the c.m.s. of the reaction $3 + x \rightarrow 2 + z$. The quantities γ^2 and κ pertain to the nuclear vertex

$$A \rightarrow 1 + 3, \quad (3)$$

γ^2 is the reduced vertex part [6] and determines the probability of the virtual disintegration (3), while $\kappa = \sqrt{2m_{13}\varepsilon}$, $\varepsilon = m_1 + m_3 - m_A$. The factor M is determined by the structure of the triangle graph.

We will also need the differential cross section $d^2\sigma/d\Omega dW$ for comparison with experimental data. It can be obtained from Eq.(2) in the following manner:

$$\frac{d^2\sigma}{d\Omega dW} = \frac{W p_x p_z^2}{2\pi E_0 |p_z - \frac{E_z}{E_0} p_x \cos \theta|} \frac{d^2\sigma}{dW dq^2} \quad (4)$$

where θ is the angle between particles z and x and E_0 is the total energy of all particles in lab. system.

We shall henceforth focus our attention on the quantity M which determines the behaviour of differential cross section (2) as function of kinematical variables (1). It is convenient to introduce dimensionless variables [7]

$$\xi = \frac{m_2}{m_3} \frac{m_A}{m_4 + \dots + m_n} \frac{W - m_1 - m_2}{\varepsilon} \quad (5)$$

$$\lambda = \frac{m_1^2}{(m_1 + m_2)^2} \frac{q^2}{\kappa^2}$$

In terms of these variables M can be expressed in the form of two-fold integral in momentum space

$$M = \frac{1}{\kappa} \int_0^\infty \int_{-1}^1 \frac{F_l(\kappa x) x^2 dx P_l(z) dz}{(1+x^2)(x^2 + \lambda - \xi - 2x\sqrt{\lambda}z - i\eta)} \quad (6)$$

with $x = p/\kappa$. Here $F_l(p)$ is the form factor of the vertex $A \rightarrow 1 + 3$, normalized by the condition $F_l(i\kappa) = 1$, l is the angular momentum of the relative motion of particles 1 and 3 in the nucleus A, P_l is the Legendre polynomial.

In practice it is needed to use the general formulas taking into account the realistic nuclear form factor. In this case it is simpler to make transformation to the coordinate space where M can be expressed as one-fold integral [4]

$$M = \frac{i^l}{2\pi} \int_0^\infty \Psi(r) j_l(\sqrt{\lambda}\kappa r) \exp(-A\kappa r + iB\kappa r) r dr. \quad (7)$$

Here j_l is the spherical Bessel function, the quantity $\Psi(r)$ is introduced by the equation

$$\Psi(r) = 4\pi i^l \int_0^\infty \frac{F_l(p)}{p^2 + \kappa^2} j_l(pr) p^2 dp \quad (8)$$

(in the single-particle model it would be proportional to the wave function of the relative motion of particles 1 and 3). The quantities A and B are defined in the following manner

$$B = \sqrt{\xi}, \quad A = 0 \quad \text{at} \quad \xi \geq 0 \quad (9)$$

$$A = \sqrt{-\xi}, \quad B = 0 \quad \text{at} \quad \xi < 0,$$

Hereinafter, except Section 5, we will take the amplitude of the lower vertex of Fig.2e to be constant as we are first of all interested in the effects due to the structure and analytical properties of the graphs. We would like, whenever possible, to obtain model independent results. Taking into account that there are no reliable data on sigma–nuclear interactions, we prefer not to rely on the calculations using a Σ –A optical potential. Let us point to the detailed research of K^- – ^4He interactions with various kinds of such potential [8]. In particular it shows a strong dependence of the results on the potential parameters.

The amplitude M (6) of Fig.2e graph has two types of singularities in W : (i) normal threshold at $W = m_1 + m_2$, and (ii) so–called triangle singularity of logarithmic type which is situated in complex plane. The position of the triangle singularity depends on the value of q^2 . In terms of the variables ξ and λ the triangle singularity is situated at

$$\xi_\Delta = \lambda - 1 + 2i\sqrt{\lambda}. \quad (10)$$

If we can approach closely to the position of the triangle singularity in an experimental investigation then the amplitude of a triangle graph would be

a sharp function and it is possible to expect that a bump in W distribution will appear. The position and width of the bump must vary with q^2 . We will discuss in Section 5 how this property of a triangle graph can be checked.

3 Procedure

Though the data [1] on the processes

$${}^9\text{Be}(\text{K}^-, \pi^+) \quad (11)$$

and

$${}^9\text{Be}(\text{K}^-, \pi^-) \quad (12)$$

(see Fig.1) do not show any narrow structures, they, as we shall see below, contain a lot of a physical information and unexpected features (positions of bump maxima, an absence of narrow nearthreshold peaks due to channels with $\Sigma \rightarrow \Lambda$ conversion and so on). The channel (11) is related to Σ^- production on the protons

$$\text{K}^- \text{p} \rightarrow \pi^+ \Sigma^- \quad (13)$$

and the channel (12) can be realized on the protons

$$\text{K}^- \text{p} \rightarrow \pi^- \Sigma^+ \quad (14)$$

as well as on the neutrons

$$\text{K}^- \text{n} \rightarrow \pi^- \Sigma^0. \quad (15)$$

The cross section of the process (14) is much less than the cross section of the process (15) at 600 MeV/c [2]. The data for the channels (11) and (12) are quite different. The main reason, evidently, is very small binding

energy of the outer neutron in ${}^9\text{Be}$ which is equal only 1.67 MeV. So it is interesting to isolate the part of the channel (12) cross section which takes place on the outer neutron.

Zero in the excitation energy E_{ex} in the channel (11) corresponds to the invariant mass W of the final state consisting from Σ^- plus the ground state of ${}^8\text{Li}$ without relative motion and in the channel (12) it corresponds to Σ^0 plus the ground state of ${}^8\text{Be}$. So $E_{\text{ex}} \geq 0$ for events with Σ -hyperon in a final state. Left parts of the spectra in Fig.1, related to $E_{\text{ex}} < 0$, can have their origin in the process of Σ production followed by the conversion



as well as (for the channel (12)) in the “tail” of direct Λ production. The estimation of this tail behaviour in the model of a quasi-free Λ production shows its sharp decrease in the interval of E_{ex} from -20 MeV to zero. It contradicts the data on the channel (12). Therefore we take the model of a quasi-free Λ production followed by its rescattering. It leads to the result shown by the solid curve in Fig.1 (the normalization of the curve is fixed by the experimental point at $E_{\text{ex}} = -20$ MeV). In the following the corresponding values (the physical background due to the direct Λ production) will be subtracted from the data for the channel (12).

The nucleus ${}^9\text{Be}$ has most probably a cluster structure which consists of the core (${}^8\text{Be}$ or two α -particles) and the loosely bound outer neutron. So the reaction (12) can have a contribution from four protons and four neutrons of the core as well as from the outer neutron. The reaction (11) can proceed only on four core protons. We have simultaneously the data on both channels (11) and (12). It provides a possibility to isolate the part of the cross section of the channel (12) which is related to the outer neutron contribution considering that the wave functions of the core neutrons and

protons are close. For this purpose let us note that the sum of the cross sections of the processes (14) and (15) at 600 MeV/c is approximately equal to 90 % of the cross section of the process (13). Thus we can believe that the contribution of the core neutrons and protons to the cross section of the channel (12) is approximately 90 % of the cross section of the channel (11). Then the expression $(\sigma_2 - 0.9\sigma_1)$ gives the contribution of the outer neutron to the cross section of the process (12). Here σ_2 is the cross section of the channel (12) minus the contribution of the tail from the direct Λ production. In the following we will compare the results of our calculations of the process (12) with the result of this very difference procedure (see the points in Fig.4a).

In subsequent calculations we will use the wave function (form factor) of the outer neutron in ${}^9\text{Be}$ from the n- α - α cluster model [9]. The corresponding form factor for the core proton was not calculated in the cluster model of ref.[9]. At the first stage we will use the p-wave oscillator wave function with the parameter $p_0 = 130$ MeV/c [10]. For studying a sensitivity of the results to a shape of a wave function we will also make calculations with the model p-wave function of a “quasi-Hulten” type

$$\psi(r) \sim \left(\frac{1}{\kappa r} + \frac{1}{\kappa^2 r^2} \right) (e^{-\kappa r} - 3e^{-(\kappa+\rho)r} + 3e^{-(\kappa+2\rho)r} - e^{-(\kappa+3\rho)r}) \quad (17)$$

which has correct asymptotic behaviour at $r \rightarrow 0$ and $r \rightarrow \infty$. Note at once that it will not change the results qualitatively.

Let us present at first several intermediate results for the case of the reaction (11) at 600 MeV/c for small angles. Fig.3a shows the real and imaginary parts of the triangle graph with a secondary interaction of the Σ -hyperon with the residual nuclear system (Fig.2b and 2c) as functions of E_{ex} . As was earlier mentioned, the calculations were carried out with constant amplitude of a secondary interaction in order to clear up at the

first place what is given by the structure of the graphs. Fig. 3b demonstrates the modulus squared of the triangle graph amplitude. We can see that it has a sharp peak near $E_{\text{ex}} = 0$ with the width about 15 MeV. The cross section of the graph of Fig.2b process includes the phase space factor proportional to $\sqrt{E_{\text{ex}}}$ and it leads to the smoothing and shifting of the peak. It is not the case for the process with the conversion (16) and the corresponding peak must be present also in its cross section. Note that the peak of the same nature is well known for the process (K^-, π^-) on the deuteron [11]. The cusp structures are also distinctly seen in the results of calculations of stopped and in-flight K^- interactions with He^4 [8,12].

The solid curve of Fig.3c shows the shape of E_{ex} distribution corresponding to the quasi-free Σ production (the pole graph of Fig.2a). The dotted curve shows the same for the triangle graph of Fig.2b. We see that both the pole graph and the triangle graph separately lead to the bumps with the width $30 \div 40$ MeV but with maxima in the region of 10 MeV and it contradicts the experimental data. However, the amplitudes of the graphs of Fig.2a and 2b interfere with each other. Comparison of the real and imaginary parts of the triangle graph in Fig.3a indicates that its phase varies sharply with E_{ex} and the result of above mentioned interference must be nontrivial. The dashed and dash-dotted curves in Fig.3c are the results of calculations for the sum of the graphs of Fig.2a and 2b with the relative phase equal to 0.4π and 0.9π respectively. They show that the position and the shape of the resulting peak may be varied over a wide range by means of relative phase variation. (Note that this phase is not known a priori as it is essentially determined by the phase of the elastic Σ -nucleus scattering amplitude and by the possible energy variation of the phases of the elementary processes (13)–(15)). Large interference effects

were also noted in ref. [8].

4 Results

Let us pass to the presentation of the results for the best fit to the data on the channels (11) and (12). First of all we are interested in a principal possibility of the description without the introduction of Σ -nuclei. Therefore at this point we did not set a task to estimate the absolute values of cross sections (at least it demands to account additionally for the absorption in initial and final states) but were concentrated on the description of the shape of the E_{ex} distributions at small pion angles. For this reason the normalization factors of Fig.2a and 2b graphs and their relative phase were taken as free parameters. Here it is necessary to make a few notes. As to an absolute normalization, ref. [8] shows that the theoretical calculations for ${}^4\text{He}$ case lead to the reasonable results when accounting of kaon and pion waves absorption. Relative contribution and phase of Fig.2b graph now cannot be evaluated reliably due to a lack of information on sigma-nuclear interactions. It is possible to put the inverse task about deriving an information on sigma-nuclear interaction from outcomes of a comparison of calculations with experimental data. It, however, is a theme of an independent research.

The solid curve of Fig.4a shows the result of the calculation for the sum of Fig.2a and 2b graphs with the relative phase 1.3π for the reaction ${}^9\text{Be}(\text{K}^-, \pi^+)$. It agrees with the data very well. The dashed curve corresponds to the "switching-off" the triangle graph of Fig.2b, i.e. presents the separate contribution of the quasi-free Σ production (Fig.2a). The contribution of Fig.2c graph was not taken into account as the experimental points at $E_{\text{ex}} < 0$ are practically equal to zero.

Fig.4b deals with the difference data for the reaction ${}^9\text{Be}(\text{K}^-, \pi^-)$ which have their origin in the process on the outer neutron (see the preceding section). The dotted curve shows the supposed contribution from the process with the conversion $\Sigma \rightarrow \Lambda$ (Fig.2c). Essentially it is analogue of the curve of Fig.3b normalized to the point at $E_{\text{ex}} = 0$ where the contributions of Fig.2a and 2b processes go to zero. The solid curve is the result of a full calculation with account of the interference of Fig.2a and 2b graphs with the relative phase 1.9π . The dashed curve is the separate contribution of the quasi-free process. We notice that the cross section of the process (12) on the outer neutron has the appearance of the peak in E_{ex} with a maximum in the region of $8 \div 10$ MeV, the width of $15 \div 20$ MeV, and can be very well described by the combination of Fig.2a–2c graphs.

Having obtained the good results for the production of Σ -hypernuclear systems on ${}^9\text{Be}$, we pass now to the description by the same method of the new data on the reaction ${}^4\text{He}(\text{K}^-, \pi^+)$ at 600 MeV/c [13]¹ and on the reaction ${}^{12}\text{C}(\text{K}^-, \pi^+)$ at 715 MeV/c [14]. For ${}^4\text{He}$ we use the s-wave oscillator wave function with the parameter $p_0 = 90$ MeV/c which gives the best fit to the data on the process ${}^4\text{He}(\text{e}, \text{ep}){}^3\text{H}$ [15]. For ${}^{12}\text{C}$ we use the p-wave oscillator wave function with the parameter $p_0 = 80$ MeV/c which gives the best fit to the data on the reaction ${}^{12}\text{C}(\text{e}, \text{ep})$ in the ground and low lying states of ${}^{11}\text{B}$ [16]. The results are shown in Fig.5a for ${}^{12}\text{C}$ and in Fig.5b for ${}^4\text{He}$. Here the dotted curves are the contributions of the processes with the conversion normalized to the points at $E_{\text{ex}} = 0$. The solid curves present the results of full calculations with account of the interference of Fig.2a and 2b graphs with the relative phase equal to

¹We will not consider now the process ${}^4\text{He}(\text{K}^-, \pi^-)$ where the bound Σ -hypernuclear state of ${}^4\text{He}$ was discovered [13]. Here the picture is more complicated due to presence of a resonance peak. In principle, our model must describe the background including, in particular, all data at $E_{\text{ex}} > 0$. We hope to discuss it in another publication.

0.9 π for Fig.5a and 1.3 π for Fig.5b. The dashed curves are the separate contributions of the quasi-free Σ production. One can see that our simple model provides a possibility to describe the data very well.

Certainly, owing to use of large number of fitting parameters our description of the data on (K^-, π^\pm) reactions can be considered simply as a successful parametrization. However, the possibility of such parametrization was not obvious beforehand. We shall note that in sigma-nuclear physics the use of large number of free parameters is not the unusual fact. Let us indicate, for example, the paper [12] where four parameters were used for the description of stopped K^- interaction with ${}^4\text{He}$.

It is necessary to emphasize also the following. In our calculations it was supposed that the residual nuclear system is in the ground state or in one of low excited states. There is direct experimental data on the reaction (e, ep) for the cases of ${}^4\text{He}$ and ${}^{12}\text{C}$. They indicate that the vertices of virtual break-up of these nuclei to proton and ground states of t and ${}^{11}\text{B}$ give dominant contribution [17,18]. The same is also noted for ${}^{12}\text{C}$ case in ref. [19] devoted to the quasifree Σ production in (K^-, π^+) reactions. There are no electron data on the vertex ${}^9\text{Be} \rightarrow n + {}^8\text{Be}$. However the evaluation in $(2\alpha + n)$ model [9] shows a preference of the transition to the ground state of ${}^8\text{Be}$. Apparently, it is not so for the process ${}^9\text{Be}(K^-, \pi^+)$. This case will be separately considered in the following section.

5 The case of ${}^9\text{Be}(K^-, \pi^+)$ reaction

E_{ex} distribution for ${}^9\text{Be}(K^-, \pi^+)$ reaction sharply differs from other cases in two aspects: (i) its maximum is shifted rightwards to $25 \div 30$ MeV, whereas in all remaining cases it is located near 10 MeV; (ii) it contains very few events at $E_{\text{ex}} \leq 0$ and practically does not leave a place

for the contribution of the narrow nearthreshold peak of Fig.3b. So the description, presented in Fig.4a, was obtained without the contribution of the conversion process and used a certainly too large value for the oscillator parameter $p_0 = 130 \text{ MeV}/c$. On the other hand, proceeding from known values of the cross sections of the elementary processes $\sigma(\Sigma^- p \rightarrow \Sigma^- p)$ and $\sigma(\Sigma^- p \rightarrow \Lambda n)$, each of which is about 150 mb in Σ momentum region $100 \div 200 \text{ MeV}/c$, it is possible to evaluate that the cross sections of the processes of conversion and elastic Σ^- rescattering should be of the same order as the cross section of the quasi-free production.

The situation with the contribution of the conversion process could be explained by supposition that the secondary Σ interactions in the lower vertices of Fig.2b and 2c graphs proceed mainly in p-wave. It results in smoothening of the nearthreshold peak and shifts it to the right [20]. However this explanation does not seem natural as there are no reasons for the special behaviour just in the ${}^9\text{Be}(\text{K}^-, \pi^+)$ case. More logical is other explanation. It is probable that continuum states of the residual nuclear system ${}^8\text{Li}$ dominate in the break-up vertex ${}^9\text{Be} \rightarrow p + {}^8\text{Li}$. Contrary to the ${}^4\text{He}$ and ${}^{12}\text{C}$ cases, there are no high resolution data on ${}^9\text{Be}(e, ep)$ reaction. It is possible only to state that the available data [21] show a wide distribution with respect to the proton removal energy and do not contradict such hypothesis. In that case, on the one hand, the E_{ex} distribution from the quasi-free Σ production is shifted to the right. On the other hand, the intermediate state in Fig.2c graph becomes not two-particle but three- or many-particle. It completely changes the shape of nearthreshold behaviour. Fig.6 shows the comparison of $|M|^2$ for the triangle graphs with two-particle (solid curve) and three-particle (dotted curve) intermediate states. The character of the dotted curve leaves room for the significant

contribution of the conversion, keeping small number of events at $E_{\text{ex}} \leq 0$. Fig.7 shows an example of successful description of ${}^9\text{Be}(\text{K}^-, \pi^+)$ data with considerable contribution of the conversion process (dotted curve). Here the dashed curve is the separate contribution of the quasi-free Σ production. Solid curve is the summary result with account of Fig.2a and 2b graphs interference, relative phase being 0.35π . The value of the oscillator parameter $p_0 = 115 \text{ MeV}/c$ was used. It is close to the value $110 \text{ MeV}/c$ which is suggested in ref. [21] for the region of large proton removal energies.

6 Moving singularities and the mechanism of Σ -hypernuclear systems production

Strictly speaking, the good description of the data on the (K^-, π^\pm) processes in the Σ -hypernuclear region by the simplest mechanisms does not exclude a possible contribution from Σ -hypernuclei. For a complete and unambiguous solution of the reaction mechanism problem it seems efficient to use the theoretical predictions which follow from the picture of moving complex triangle singularities described in Section 2. As mentioned above, the presence of these singularities near the physical region of a reaction must lead to a maximum in E_{ex} distribution. The position and the shape of the bump must change with the momentum q transferred from the initial kaon to the final pion [5]. Numerical calculations should show whether this effect is noticeable or not. The contribution of the quasi-free Σ -hyperon production would conceal the above mentioned effect. Therefore it is desirable to study it in the channels with the conversion $\Sigma \rightarrow \Lambda$ (i.e. with the detection of Λ) where Fig.2a graph does not make a contribution. To investigate the discussed picture one needs to measure the

differential cross section $d^2\sigma/dE_{\text{ex}}dq^2$, which is directly expressed through the modulus squared of the matrix element (see Eq.(2)), in a wide range of E_{ex} and q .

For example, let us consider the reaction $^{12}\text{C}(\text{K}^-, \pi^+)$. Fig.8a shows the theoretical predictions for the modulus squared of the Fig.2c graph amplitude as a function of E_{ex} for different values of $q= 200, 250, 300, 350$ MeV/c. A distinct picture of the moving and the broadening of the peak is visible. This picture is quite available for an experimental observation.

The question is what would happen with the same distributions in the case of Σ -hypernucleus production (the graph of Fig.2d)? To answer the question, calculations were made with inclusion of a resonance state (a Breit-Wigner pole was put in) with the width of 10 MeV and the mass which was 15 MeV more the sum of the masses of Σ and the ground state of residual nucleus. Fig.8b shows the results for the same set of the momentum transfer. As could be expected, the position of the maximum remains practically constant in this case. It follows that the investigation of $d^2\sigma/dE_{\text{ex}}dq^2$ would make it possible to answer unambiguously the question about the nature of the irregularities in the excitation energy spectrum of the processes (K^-, π^\pm) : whether they are due to the reaction mechanism or to the existence of Σ -hypernuclei.

7 Conclusion

Thus all considered data on the reactions (K^-, π^\pm) in the Σ -hypernuclear region can be basically described without the supposition on the existence of Σ -hypernuclei. The bumps in the excitation energy distributions of the residual nuclear systems are due to the peculiarities of the reaction mechanisms.

The successful description of the available data by means of the simplest mechanisms cannot completely exclude the existence of hypernuclei. We tried to emphasize that the decisive conclusion on this problem can be made only with the help of a detailed investigation of the Σ -hypernuclear system production mechanism. We propose to study the cross section $d^2\sigma/dE_{\text{ex}}dq^2$ at different values of momentum transfer q , as its behaviour strongly depends on the existence of Σ -hypernuclei. If the experimental investigations will confirm the picture of moving singularities, predicted in Section 5, and thus the dominant contribution of the Fig.3c graph in the channels with the conversion, then it would be possible to extract the cross section σ_{12} of the Σ -nucleus interaction using Eq.(2). In the future this value of σ_{12} could be compared with dynamical calculations.

Note that the considered picture of moving singularities of triangle Feynman graphs in the case of rescattering effects for Σ -hypernuclear systems production is universal one. The same phenomena could be observed at different kinematical conditions in other reactions, for instance $A(e, e'K^-)X$.

The authors are indebted to Prof. I.S.Shapiro for the attention to the investigation and discussions, to Profs. T.Nagae and R.E.Chrien for information on the experimental data and to Profs. V.I.Kukulin, V.I.Pomerantsev and M.A.Zhusupov for the advices and the data on the neutron form factor of ${}^9\text{Be}$.

References

- [1] R.Sawafta, Nucl.Phys. A585 (1995) 103.
T.Nagae, Abstracts of 25th INS Intern. Symposium (Tokyo, Dec.1996), p.130. Nuclear and Particle Physics with High-Intensity Proton Accelerators, ed. T.Komatsubara et al. (World Scientific, 1998) p.265.
- [2] C.B.Dover, D.J.Millener, A.Gal, Phys.Rep. 184 (1989) 1.
- [3] L.N.Bogdanova, V.E.Markushin, Particles and Nuclei 15 (1984) 808.
- [4] O.D.Dalkarov and V.M.Kolybasov, Sov.J.Nucl.Phys. 18 (1974) 416.
- [5] O.D.Dalkarov, V.M.Kolybasov and D.V.Voronov, Preprint of Lebedev Physical Institute no.8 (1995).
- [6] I.S.Shapiro, Sov.Phys.Uspekhi 10 (1967) 515.
- [7] E.I.Dubovoj and I.S.Shapiro, Sov.Phys.JETP 24 (1967) 839.
- [8] T.Harada and Y.Akaishi, Progr.Theor.Phys. 96 (1996) 145.
- [9] V.T.Voronichev, V.I.Kukulin et al. Yad.Fiz. 57 (1994) 1964.
M.A.Zhusupov et al. Izvestiya of Russian Academy of Sciences, ser. Physica 58 (1995) 55.
- [10] F.Ajzenberg-Selove, Nucl.Phys. A490 (1988) 1.
- [11] T.H.Tan, Phys.Rev.Lett. 23 (1969) 395.
R.H.Dalitz, Strange particles and strong interactions (Oxford University Press) 1962.
A.E.Kudryavtsev, JETP Letters 14 (1971) 137.
- [12] R.H.Dalitz and A.Deloff, Nucl.Phys. A585 (1995) 303c.

- [13] T.Nagae et al., Phys.Rev.Lett. 80 (1998) 1605.
- [14] L.G.Tang et al. Phys.Rev. C38 (1988) 846.
- [15] J.M.Laget, Nucl.Phys. A497 (1989) 391c.
- [16] G. van der Steenhoven et al., Nucl.Phys. A480 (1988) 547.
- [17] J.F.J. van den Brandt et al., Phys.Rev.Lett. 60 (1988) 2006.
J.M.Le Goff et al., Phys.Rev. C50 (1994) 2278.
- [18] J.Mougey et al. Nucl.Phys. A262 (1976) 461.
- [19] R.E.Chrien et al. Phys.Rev. C35 (1987) 1589.
- [20] V.M.Kolybasov, Preprint of Lebedev Physical Institute no. 42 (1997);
Physics of Atomic Nuclei, in print.
- [21] V.A.Goldshtein et al., JETP Letters 19 (1976) 695.
E.L.Kuplennikov et al., Yad.Fiz. 25 (1977) 1129.

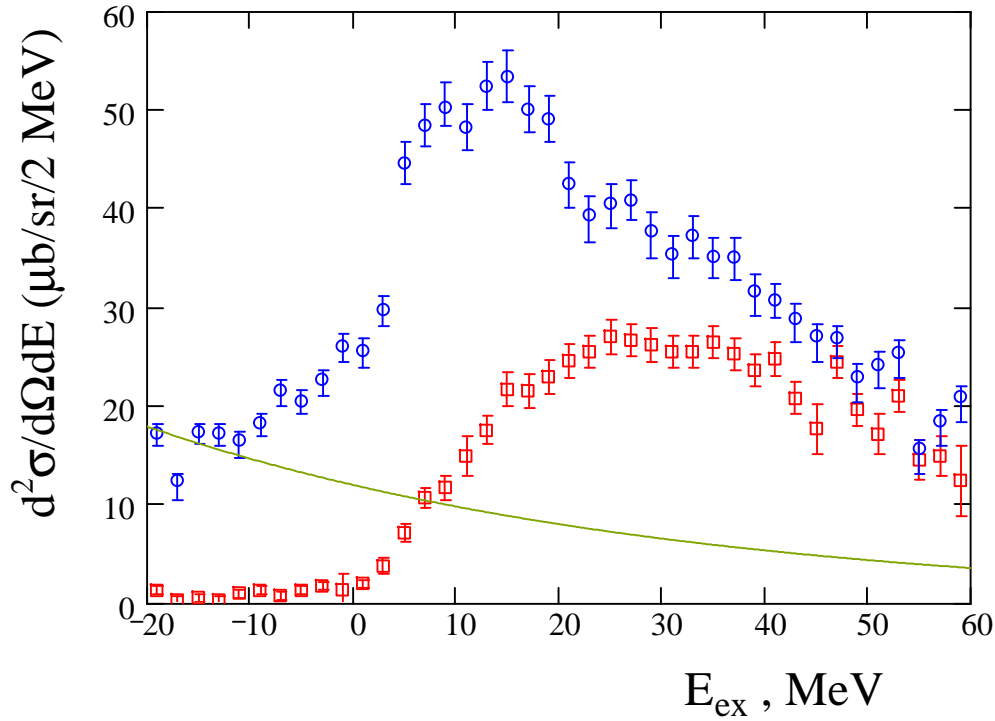


Figure 1: The data of ref.[1] on the differential cross sections of the reactions ${}^9\text{Be}(K^-, \pi^-)$ (circles) and ${}^9\text{Be}(K^-, \pi^+)$ (squares) at small angles at 600 MeV/c. The solid curve is the approximation of the tail of direct Λ production used in Section 3.

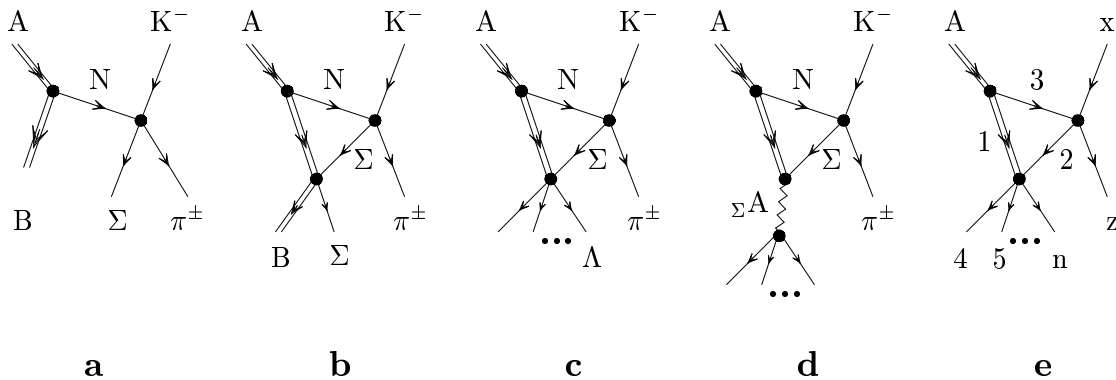


Figure 2: The graphs for the processes (K^-, π^\pm) on nuclei (a–d) and a generic form of the triangle graph (e).

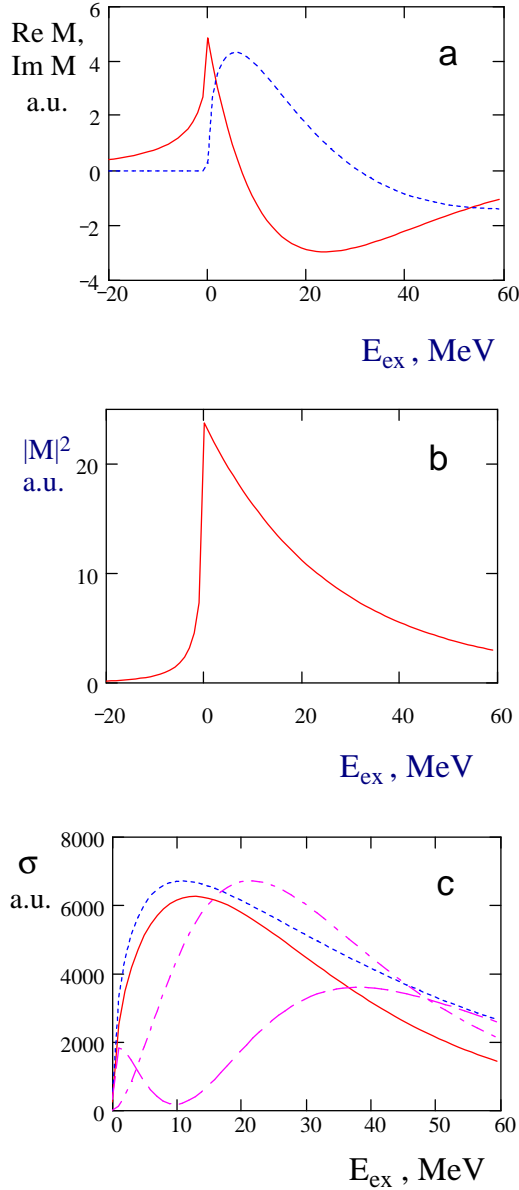


Figure 3: The results of intermediate calculations for the process ${}^9\text{Be}(\text{K}^-, \pi^+)$: (a) real and imaginary parts of the triangle graph amplitude; (b) modulus squared of the triangle graph amplitude; (c) the shapes of the contributions to the cross section from the quasi-free Σ production of Fig.2a (solid curve), from the Fig.2b triangle graph (dotted curve) and from two versions of the account of the interference of the Fig.2a and 2b graphs with the relative phase 0.4π (dashed curve) and 0.9π (dash-dotted curve).

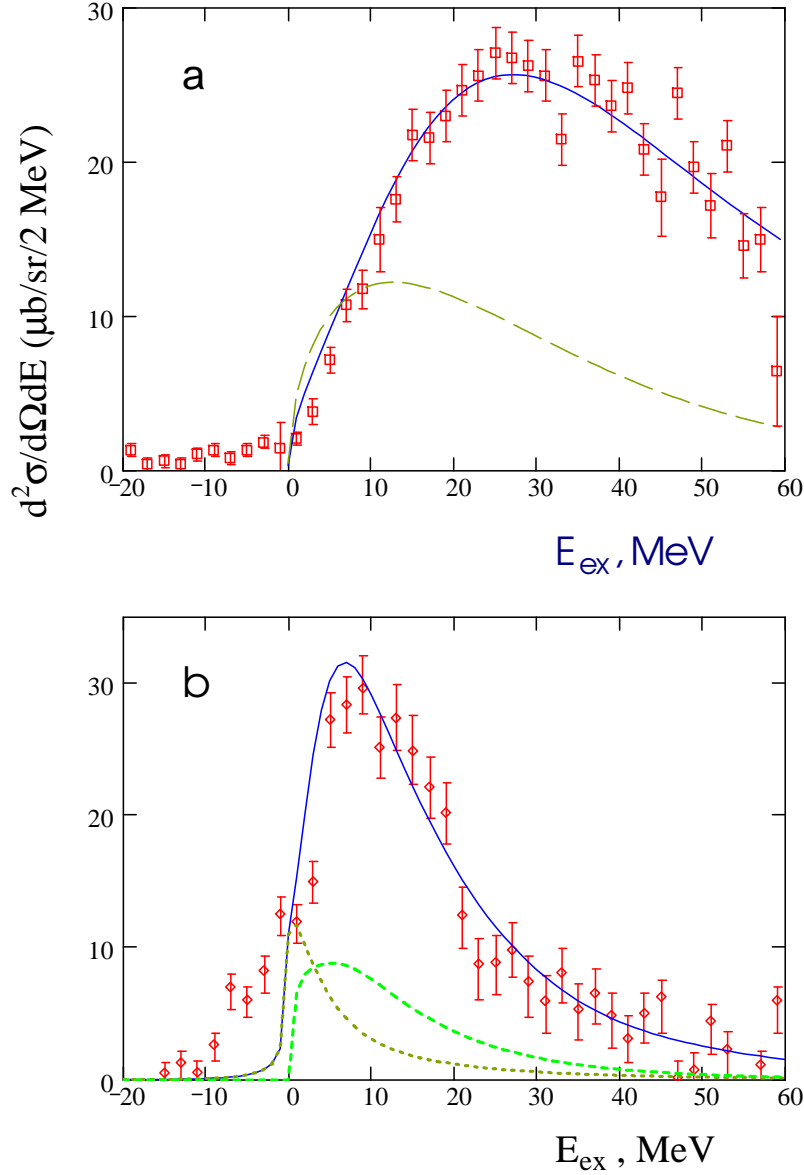


Figure 4: (a) The excitation energy distribution in the reaction ${}^9\text{Be}(\text{K}^-, \pi^+)$. The data are from ref.[1]. The solid curve is the result of a full calculation. The dashed curve shows the contribution only from the quasi-free Σ production (Fig.2a). (b) The excitation energy distribution in the reaction ${}^9\text{Be}(\text{K}^-, \pi^-)$ on the outer neutron. The experimental data are obtained from the data of ref.[1] by means of the difference procedure described in Section 3. The solid curve is the result of a full calculation. The dotted curve is the contribution of the processes with the conversion $\Sigma \rightarrow \Lambda$. The dashed curve shows the contribution only from the quasi-free Σ production (Fig.2a).

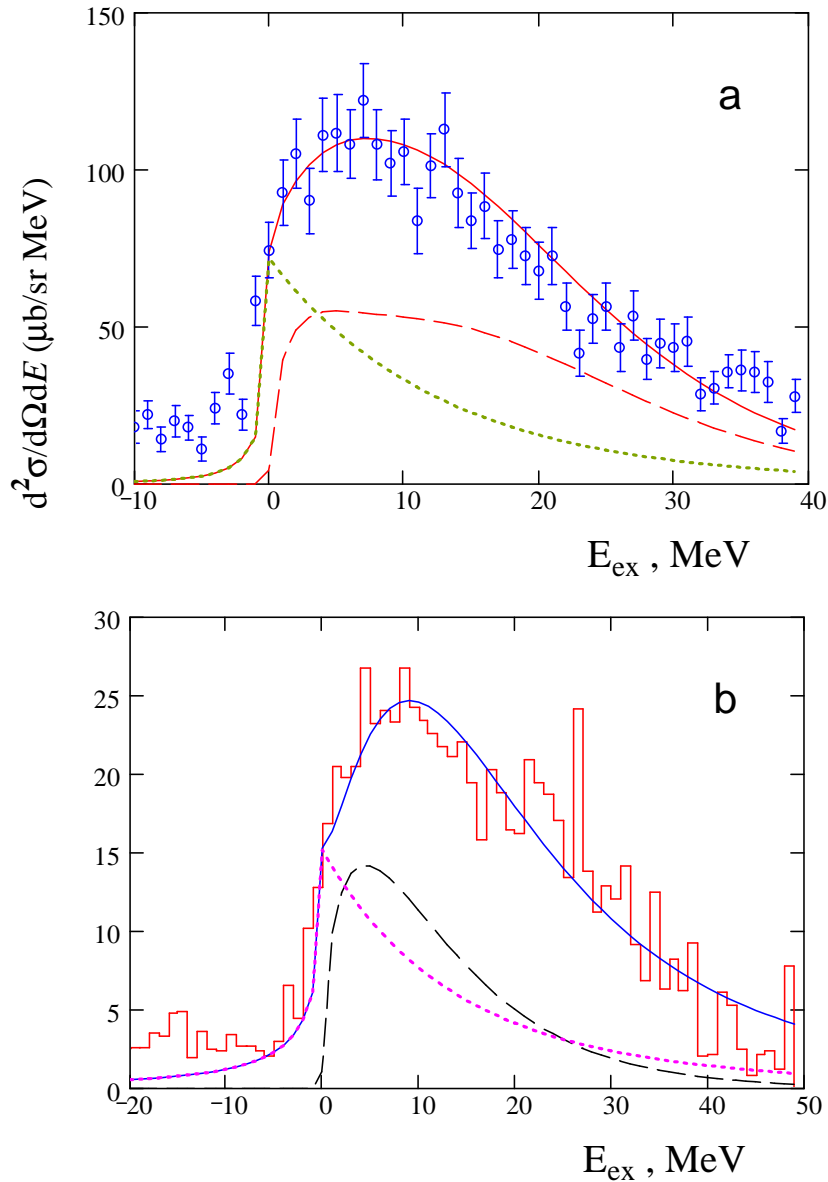


Figure 5: (a) The excitation energy distribution in the reaction $^{12}\text{C}(K^-, \pi^+)$ at 715 MeV/c for 4° . The data are from ref.[12]. The solid curve is the result of a full calculation. The dashed curve shows the contribution only from the quasi-free Σ production (Fig.2a). (b) The excitation energy distribution in the reaction $^4\text{He}(K^-, \pi^+)$ at 600 MeV/c for small angles. The experimental histogram is from ref.[11]. The meaning of the curves is the same as in Fig.5a.

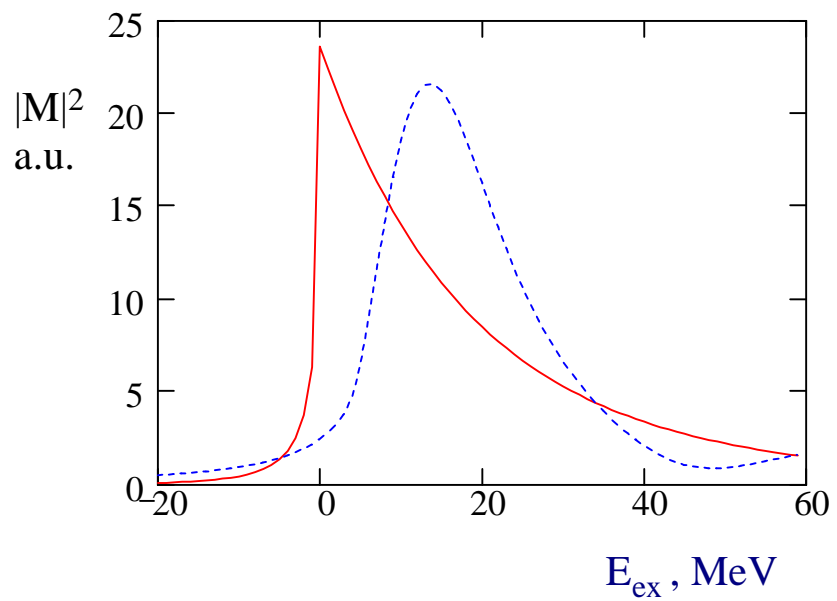


Figure 6: $|M|^2$ for the triangle graph of Fig.2c with two-particle (solid curve) and three-particle (dotted curve) intermediate states.

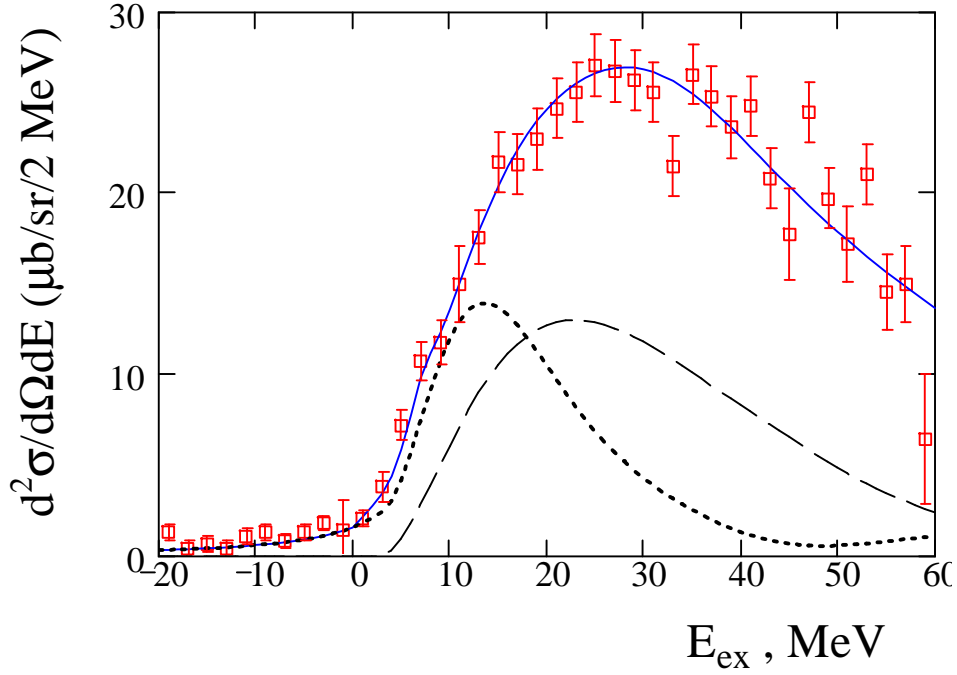


Figure 7: The excitation energy distribution in the reaction ${}^9\text{Be}(\text{K}^-, \pi^+)$ with three-particle intermediate state in Fig.2c graph. The solid curve is the result of a full calculation. The dotted curve is the contribution of the processes with the conversion $\Sigma \rightarrow \Lambda$. The dashed curve shows the contribution only from the quasi-free Σ production.

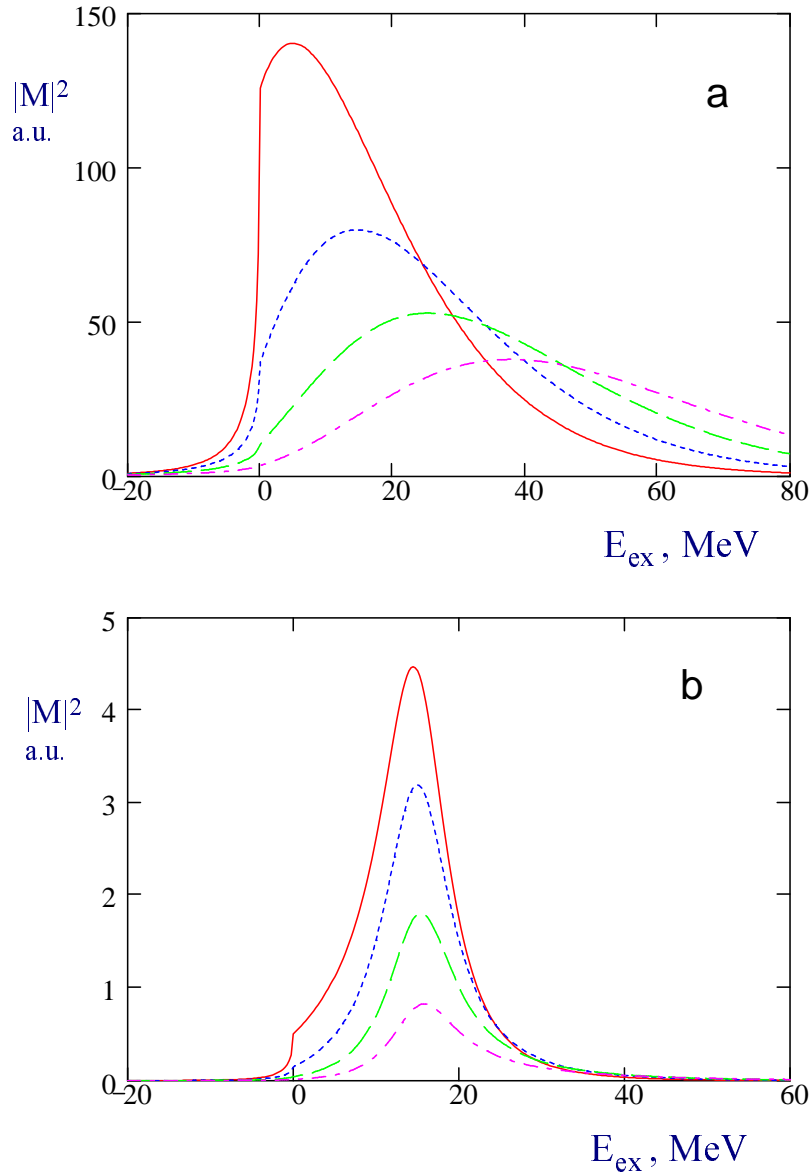


Figure 8: (a) The modulus squared of the Fig.2c graph amplitude for the reaction $^{12}\text{C}(\text{K}^-, \pi^+)$ at different values of the momentum transfer $q = 200$ MeV/c (solid curve), 250 MeV/c (dotted curve), 300 MeV/c (dashed curve) and 350 MeV/c (dash-dotted curve). (b) The same with the inclusion of the excited Σ -hypernuclear state (Fig.2d) with the width 10 MeV and the mass corresponding to $E_{\text{ex}} = 15$ MeV.